The Kinetics of Ion Exclusion

BASIL VASSILIOU and JOSHUA S. DRANOFF

Northwestern University, Evanston, Illinois

As a preliminary to detailed kinetic analysis of ion-exclusion operations a study of the rate of absorption of glycerol from dilute aqueous solution has been made in small fixed beds of ion exchange resin. The resin used was Amberlite IR-120 (hydrogen form) ranging in size from 0.210 to 1.190 mm., as determined by dry screening. Solution flow rates were varied from 0.45 to 22.20 ml./(sq.cm.min.).

Analysis of this problem has shown that the operation of such a process may be described by a simple linear rate equation and the usual transient column material balance relations. It was found that experimental breakthrough data could be well matched with curves predicted by such analysis. Furthermore, three characteristic regions of operation are apparent in which different rate controlling processes may be operating.

Ion exclusion is a process for the separation of ionic and nonionic solutes present in a polar solvent by the use of ion exchange resins. It shows promise of becoming an important industrial tool because it is relatively simple and inexpensive.

In ion exclusion, as contrasted with standard ion exchange separations, the nionionic component is preferentially removed from solution by the resin and is later recovered by elution with the original solvent. The process depends on the fact that solutes tend at equilibrium to be distributed at different concentrations in the solution which surrounds an ion exchange particle and which is present within the resin structure. Nonionized solutes are normally found at higher concentration within the particle than ionized materials, especially with the high capacity, strongly ionized resins now in common use. Such behavior may be explained in terms of Donnan Membrane equilibrium theory, as summarized by Kunin (*6*), which may be considered to be the basis for ion-exclusion effects. The preferential exclusion of the ionic component from the resin makes possible the use of ion exchange resins for chromatographic separations in such systems.

The application of ion exclusion has received moderate attention since the early work of Wheaton and Bauman (*20*). They, along with Simpson and Wheaton (*14*) and Simpson and Bauman (*15*), studied the general problem. They have reported data concerning the effects of principle operating parameters on the efficiency of this technique. In addition Simpson and Bauman (*15*) have presented a theory of the operation of a fixed-bed ion-exclusion column assuming that equilibrium exists throughout the equipment. Some of the primary results obtained to date have been summarized by these investigators in the book edited by Nachod and Schubert (*8*).

Many systems of organic solutes combined in aqueous solution with ionic solutes have been studied experimentally. Among those which have received the most attention is the glycerol-sodium chloride-water system. Prielipp and Keller (*11*), Asher and Simpson (*1*), Shurts and White (*13*), and Vassiliou (*17*) have reported experimental studies of the operation of ion-exclusion columns and/or basic equilibrium distribution data for this system.

Almost all the work done up to the present has been based on the assumption that the equilibrium distributions of solutes alone determine the success of such separations. Most attempts at analysis have assumed the relative distribution coefficients of the various solutes to be the most important indicator of possible separations. Little attention has been given to the possible role that the rate processes involved may play in the overall process. That this may be a significant role is underlined by the data obtained for the separation of polyethylene polyamines from sodium chloride. The highest member of the series (di-, tri-, tetra-amino compounds), tetra-ethylene pentamine, was most poorly separated from the salt solution even though it has the most favorable equilibrium distribution (*9*). It is quite possible that the relative rates of diffusion of the various solutes from external solution to the internal resin phase solutions was responsible for this behavior.

The only other study of ion exclusion reported involving the effect of kinetics is the recent work of Tayyabkhan (*16*). He has considered the equilibrium and rate aspects of the problem in some detail and has concluded that although equilibria are important in determining the general behavior of an ion-exclusion column, the rate processes must also be considered in order to obtain correspondence with experimental data. In particular he favors the use of a rate model based on diffusion of the solutes within spherical resin particles. He has been moderately successful in applying his model to some data available in the literature.

Since this area has been otherwise largely neglected, it was decided to make a detailed study of the kinetics of ion exclusion. It is hoped that this will help to elucidate the relative importance of both the equilibrium and rate aspects of the problem and thereby permit a more intelligent application of the technique to systems of interest. This paper reports the results of the first preliminary work in this area.

The glycerol-water-Amberlite IR 120 (hydrogen form) system was studied. In order to simplify the analysis the initial work was aimed at uncovering the kinetics of the *absorption* process in fixed bed columns with only the nonionized solute present.

The operation of the packed bed was analyzed and shown to be similar to other transient packed-bed processes. It was found, as reported below, that this transfer process is apparently controlled by solute diffusion and may be described by a simple linear rate equation. The dependence of this rate on external solution flow rate was determined and appears to be consistent with other mass transfer studies.

It is planned in subsequent work to treat the absorption of the ionic component alone in a similar way and eventually to combine these results in a complete analysis of realistic column operation with the total system.

THEORY

The operation of an ion exclusion column may be analyzed in general by writing the appropriate differential equations and boundary conditions which describe the basic processes occurring within the column. This may be done by combining equations which describe the equilibrium and rate processes of the absorption with the column material balance relation, taking proper note of the experimental conditions which prevail.

Consider first the equilibrium distribution which describes the ion-ex-

---

Basil Vassiliou is with Rohm and Haas Company, Philadelphia, Pennsylvania.

clusion process. It has been shown by earlier workers that one may characterize the equilibrium with an equation of the form

$$q = K_d C \qquad (1)$$

Although K_d values generally are functions of concentration, it may be assumed for some systems, such as that presently under consideration, that K_d remains essentially constant, thus producing a linear equilibrium relationship over restricted concentration ranges (*13*).

Values of K_d may be determined experimentally in fixed-bed experiments. When a solution of concentration C_o is allowed to flow over a bed initially free of solute, the effluent composition will change as shown in Figure 1. The volume V_1 is the total external void volume in the column; while V_2 is the volume at which the bed is essentially saturated with respect to the input solution. Area *B* plus *C* on this figure represents the total amount of solute fed to the column up to saturation, not including that required to flush out the external voids, area *A*. Since area *C* represents the total amount of solute recovered in the column effluent, the remainder, area *B*, is the amount held within the particles and in equilibrium with the solution of concentration C_o present in the external voids at saturation. If the volume V_1 is known, as well as the total internal volume of the particles V_{Int}, one may calculate the distribution coefficient as follows:

$$K_d = \left(\frac{q}{C}\right)_{eq} = \frac{C_o\,(V_2 - V_1) - \int_{V_1}^{V_2} C dV}{C_o} \qquad (2)$$

A similar procedure may be used to calculate K_d from elution curves.

As far as specification of the rate equation, which describes the transport of solute between external and internal solutions specifically in ion exclusion, is concerned there are no data in the literature to suggest a proper form. It was therefore assumed that one may describe this transfer operation by equations of a type which have been so successfully applied to other fixed-bed operations. In particular the following form is assumed in the present case:

$$\frac{\partial q}{\partial t} = k(K_d C - q) \qquad (3)$$

Note that this equation is consistent with the equilibrium formulation previously discussed.

The differential material balance relation for the column may be written at once after the following assumptions are made:

1. The column is packed in a uniform random fashion with granular absorbent, in this case ion exchange resin particles.
2. Solution is allowed to flow down through the bed at a fixed rate and with a constant input concentration of solute.
3. The solution flows over the cross section of the bed in uniform plug flow with negligible mixing and/or diffusion in the axial direction. Note that the neglect of axial diffusion is in accord with common practice for such problems. One would not normally expect such effects to be important for deep beds except at very low flow rates. See for example Vermeulen and Hiester (*19*).

It then follows that

$$L\frac{\partial C}{\partial z} + \epsilon\frac{\partial C}{\partial t} + f\frac{\partial q}{\partial t} = 0 \qquad (4)$$

The appropriate boundary conditions may be specified with reference to the assumptions stated before and the fact that the column is initially in a uniform condition with the internal and external volumes filled with solutions of concentration q_i and c_i. These statements are reflected in the equations

$$c(o, t) = C_o \qquad (5)$$

$$c\left(z, t \leq \frac{\epsilon}{L} Z\right) = C_i \qquad (6)$$

$$q\left(z, t \leq \frac{\epsilon}{L} Z\right) = q_i \qquad (7)$$

Note that c and q will be functions of the two variables Z and t.

The solutions to this set of equations is well known and may be shown to be

$$\frac{C - C_i}{C_o - C_i} = 1 - \int_0^{\eta} e^{-(\tau+\eta)} J_o(i\sqrt{4\tau\eta})d\eta \qquad (8)$$

$$\frac{q - q_i}{q_o^* - q_i} = \int_0^{\tau} e^{-(\tau+\eta)} J_o\,(i\sqrt{4\tau\eta})d\tau \qquad (9)$$

where

$$\eta = K_d\, k \frac{f}{L} Z \qquad (10)$$

$$\tau = k\left(t - \frac{\epsilon}{L} Z\right) \qquad (11)$$

$$q_o^* = K_d\, C_o \qquad (12)$$

These solutions have been previously determined by several investigators and are presented in graphical and tabulated form in a number of now standard references (*2, 4, 5, 10, 12*). In addition Vermeulen (*18*) has considered the linear equilibrium case in some detail and has shown that the same form of solution is to be expected for several different rate steps in that case. The solution predicts that the effluent liquid concentrations will change from the starting value C_i to the input value C_o in the general s-shaped fashion associated with experimental breakthrough curves. Furthermore the exact shape of the curve will depend primarily on the magnitude of the rate constant k defined in Equation (3). The solution equations may be used in two ways, that is either to predict the output of a given column for which all parameters are known or to calculate the value of an unknown parameter (such as k) by matching experimental and calculated breakthrough curves. In the present case the latter technique was used for the determination of the unknown rate constants.

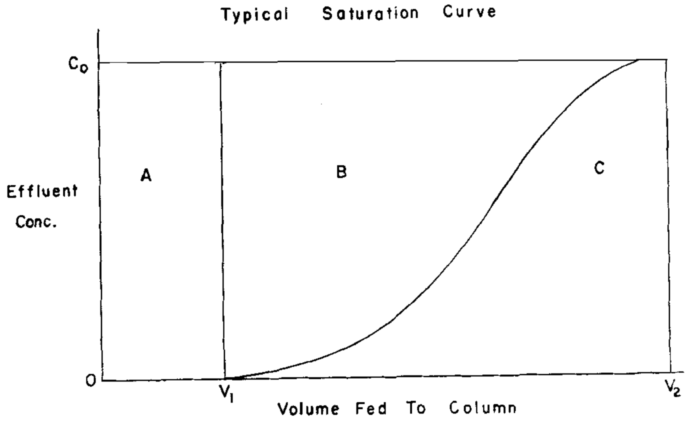

Fig. 1. Typical column saturation curve.

APPARATUS AND PROCEDURE

The absorption of glycerol from dilute water solutions (approximately 7.0 wt. % glycerol) was carried out in a simple fixed-bed unit. The column consisted of a glass cylinder 70 cm. high having an inside diameter of 1.36 cm. The resin bed was confined and supported in the column by fine stainless steel screens, and the column was fitted at either end with stopcocks for

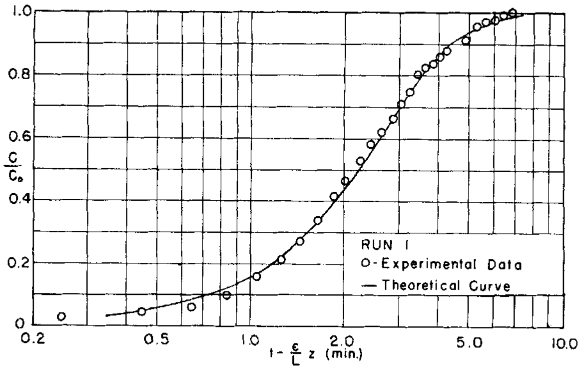

Fig. 2. A comparison of experimental and calculated data for run 1.

flow control. Glycerol solution or pure water for elution was fed to the bed under the influence of gravity from feed bottles located 1.5 m. above the top of the column.

The column was packed with Amberlite IR-120 resin (in the hydrogen form) with a cross linkage of 8 to 10% divinylbenzene. The resin used consisted of particles of a size between 420 and 590 μ as measured by dry screening between 30- and 40-mesh standard screens. A limited number of experiments were also made with particles of two other average sizes determined in the same manner. The bed was put in place by allowing the particles to settle into the column when it was filled with water. In this way uniform packing was obtained throughout the column.

The external void fraction in the column when packed was determined by saturating the bed with standard 0.1 normal hydrochloric acid and then eluting with distilled water at the highest possible flow rate, approximately 20 ml./sq. cm. min. The amount of acid eluted was measured and the resultant external void volume calculated from the concentration of the original acid. From such measurements it was found that the external void fraction was 0.40.

The internal void fraction was determined by measuring the volume of water contained within the particles that would occupy a known volume of packed bed. The particles were saturated with pure water, and after the surface water was removed from each particle with filter paper, the wet particles were weighed. The beads were then dried at 110°C. for 16 hr. and the dried particles reweighed. Repeated measurements made in this way were reproducible within 1%. The volume of internal water was then determined with the density of liquid water. The resultant calculated internal void fraction was 0.402, based on the bulk packed volume of the bed.

This equipment was used to determine the breakthrough curves in the following way. The column was first packed with the desired resin and washed thoroughly with distilled water prior to saturation runs. Standard glycerol solution was then admitted to the top of the column at a desired flow rate. Measured samples of the column effluent were taken thereafter at measured time intervals. The samples were analyzed for glycerol by determining the refractive index at 20°C. using a standard relationship between concentration and refractive index (*7*).

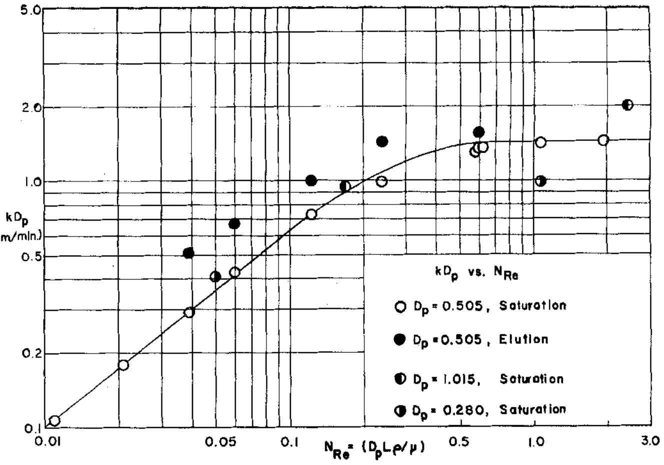

Fig. 3. $k\ D_p$ vs. Reynolds number.

Elution breakthrough curves were determined simply by washing the saturated column with distilled water and collecting and analyzing effluent samples as above.

It should be noted that there was no noticeable shrinkage or expansion of the bed observed during these experiments. This observation is in agreement with the data of Shurts and White (*13*) for sodium form resin and dilute glycerol solutions.

RESULTS AND DISCUSSION

The equipment described above was used to make sixteen saturation and elution runs with the glycerol-water-resin system. The conditions of these runs are indicated in Table 1.

The data of runs 1, 2, 3, 6, 7, and 11 were used first to determine the effect of solution concentration and flow rate on the measured distribution coefficient for glycerol in the Amberlite IR 120 resin (hydrogen form). The coefficients, as calculated from both the elution and saturation curves by the method indicated earlier, agreed within two significant figures. The results are shown in column 5 of Table 1. These data show that K_d is essentially independent of the solution flow rate used in the experiments, as would be normally expected since K_d is an equilibrium parameter. On the other hand it is evident that K_d is a slight function of solution concentration. When the solution concentration was more than doubled from run 1 to run 3, the value of K_d increased approximately 7%. Although this variation is not negligible, it is assumed for present purposes that one may reasonably represent the actual equilibrium behavior with a single value over the concentration range of interest in the bulk of these experiments, namely 0.0 to 7.05 wt. % glycerol. The value chosen for use in subsequent calculations was 0.60, which is representative of the experimentally determined values. It should be noted that this value is entirely consistent with previously reported values of 0.6 to 0.65 as reported by Bauman, Simpson, and Wheaton (*8*).

The data were then used to calculate the mass transfer coefficients de-

Table 1. Experimental and Calculated Results

Run	D_p,* (mm.)	C_o, (wt. % gly.)	L, ml./(min.) (sq. cm.)	K_d	k saturation	(min.)$^{-1}$ elution	N_{Re}
1	0.505	4.06	6.92	0.580	2.719	—	0.622
2	0.505	7.05	6.92	0.601	2.663	—	0.599
3	0.505	9.80	6.92	0.625	2.594	—	0.576
4	0.505	7.05	0.132	—	0.213	—	0.011
5	0.505	7.05	0.243	—	0.356	—	0.021
6	0.505	7.05	0.45	0.605	0.575	1.01	0.039
7	0.505	7.05	0.692	0.601	0.850	1.34	0.060
8	0.505	7.05	1.42	—	1.46	2.00	0.123
9	0.505	7.05	2.77	—	1.96	2.84	0.240
10	0.505	7.05	6.92	—	2.67	3.12	0.599
11	0.505	7.05	12.50	0.603	2.80	—	1.083
12	0.505	7.05	22.20	—	2.84	—	1.923
13	1.015	7.05	0.97	—	0.938	—	0.169
14	1.015	7.05	13.85	—	1.96	—	2.41
15	0.280	7.05	1.03	—	1.48	—	0.050
16	0.280	7.05	22.20	—	3.55	—	1.07

* Particle size range: 0.280 = 0.210 to 0.350 mm., 0.505 = 0.420 to 0.590 mm., 1.015 = 0.840 to 1.190 mm.

fined by Equation (3). The technique of matching experimental curves with those predicted by Equation (8) was used. The consistency of such solution curves and experimental data is shown for a typical run in Figure 2.

The resultant mass transfer coefficients are shown in columns 6 and 7 of Table 1. In addition the product of these coefficients and the appropriate average particle diameters have been plotted against an average Reynolds number on logarithmic coordinates in Figure 3. This form of ordinate was selected in order to account for different particle sizes. Note that the rate Equation (3) is written per unit volume of packed bed, and thus the coefficient k is similarly based on packed volume. However since the total flux of solute depends on the effective particle-solution interfacial area, data for different particle sizes must be compared in a manner which accounts for the corresponding different areas per unit volume. Since it may be easily shown that total surface area per unit volume is inversely proportional to particle diameter for small spherical particles, the $k\,D_p$ values should be directly comparable.

The Reynolds numbers in Figure 3 are based on particle diameter and superficial velocity and were calculated with operation assumed at 25°C., with values of viscosity and density corresponding to the arithmetic concentration of solution within the column during any run. Appropriate constants for these solutions were taken from standard tables (*7*).

The data shown in Figure 3 exhibit several very interesting properties.

The bulk of the data were taken for saturation runs with resin particles in the 0.505-mm. diameter range. These points, shown as open circles, are quite self-consistent and lie on a single, well-defined curve. Moreover this curve may be conveniently broken up into three distinct zones:

1. A zone for $N_{Re} \leq 0.15$, where $k\,D_p$ is proportional to $(N_{Re})^{0.74}$.
2. A transition zone for $0.15 \leq N_{Re} \leq 2.0$.
3. A zone for $N_{Re} \geq 2.0$, where $k\,D_p$ is independent of N_{Re} and equal to 1.43 (mm./min.).

The existence of three such zones is not unexpected if one considers the basic nature of the absorption process. It is clear that the mechanism of absorption may be considered as diffusion of solute from the bulk external solution to the immediate vicinity of the particle surface, followed by diffusion of the solute into the internal resin phase solution. The over-all rate of the process will depend upon the rates of these two diffusional steps. In this context zone 1 may be considered to be a region in which diffusion in the external solution is the rate-controlling process. As the N_{Re} is increased, the rate of this process is increased until both steps are of comparable importance, thus producing the transition zone 2. Further increase in N_{Re} leads to the situation in which the external transfer is so fast, relatively, that the internal diffusion becomes rate controlling. Further increases in N_{Re} will no longer have any effect on the transfer coefficient, as is evident in zone 3.

It should be noted that the dependence of $k\,D_p$ on Reynolds for low flow rates is not quite in agreement with more other packed-bed studies. Most correlations show an exponent on Reynolds number between 0.4 and 0.6, although Gilliland and Baddour (*3*) reported a value of 0.84 for a comparable coefficient in an ion exchange investigation. The value of 0.74 found in the present work is somewhat higher than usual. Although the reason for this is not immediately obvious, it is conceivable that the high exponent is due to axial diffusion, which has been neglected in the present analysis. If axial diffusion is significant, it would tend to spread out the breakthrough curve. This would result in low k values, with the effect more pronounced at low flow rates. If a suitable correction could be applied, this would result in corrected k values, which would be somewhat higher at the lower values of N_{Re}. The net effect would be thus to lower the Reynolds number exponent possibly to the range most frequently encountered by others. Future work will attempt to account for possible axial diffusion effects.

Figure 3 also shows data obtained from elution runs made with the same particles. In each case these points are higher than the saturation values. The reason for this behavior is presently obscure. However it may be due to some differences in activity of the solute in saturated and solute-free resin phases or more probably to the neglect of changes in K_d with solution concentration. Nonlinearities in this relationship may easily produce self-sharpening or spreading in the breakthrough curves, tending to cause the type of disagreement found here. The latter effect may be investigated in experiments with more dilute solutions, 1% glycerol for example, for which the assumption of constant K_d would be more valid. It is planned to consider this effect also in future work.

Finally, the data of four runs made with two other particle sizes are also shown on Figure 3. For the lower Reynolds number, where external diffusion controls the over-all rate, these data agree closely with the curve representing the particles with D_p = 0.505 mm. However at higher Reynolds numbers the data do not agree, even when compared in terms of $k\,D_p^2$. Note that the latter form might be expected to be constant under conditions of internal particle diffusion control (*18*). In view of the very limited amount of data presented here and the wide ranges of particle size represented by the average particle diameters listed in Table 1 it is not possible to state whether or not this disagreement is significant.

An attempt was made to calculate effective diffusion coefficients for glycerol in both external and internal diffusion controlled cases with the equations of Gilliland and Baddour (*3*) with the present data. Values of approximately 10^{-6} sq. cm./sec. were found for both cases. Tayyabkhan has reported values of approximately 1×10^{-5} and 5×10^{-7} sq. cm./sec. for these two cases, respectively. The present estimates lie within this range, but closer agreement would have been expected.

In view of these data it may be concluded that the rate model proposed in Equation (3) is consistent with the experimental data. Therefore one may use the fixed-bed analysis presented above to predict the behavior of an ion exchange column for the absorption of glycerol. There remain some serious questions to be answered concerning the dependence of the coefficient k on process parameters, notably the difference between saturation and elution, the effect of particle size at high Reynolds numbers, and the possible effect of axial diffusion. It is felt however that the present approach will make possible the resolution of the problem in the future. Continued effort is being directed along these lines in this laboratory, and more extensive data will be forthcoming which may help to answer these questions.

ACKNOWLEDGMENT

The support of the North Atlantic Treaty Organization in the form of a fellowship to one of the authors (Basil Vassiliou) is acknowledged with thanks.

NOTATION

C = solute concentration in external solution (milli-equivalents/ml.)
C_o = input solute concentration
C_i = initial solute concentration within the fixed bed

D_p = particle diameter (mm.)
ϵ = external void fraction (ml. fluid/ml. packed volume)
f = internal void fraction (ml. fluid/ml. packed volume)
K_d = equilibrium distribution coefficient (dimensionless)
k = mass transfer coefficient (min.$^{-1}$)
L = solution flow rate [ml./(min.)(sq.cm.)]
q = solute concentration in internal solution (milli-equivalents/ml.)
q_i = initial solute concentration within the bed
q_o^* = internal concentration in equilibrium with external concentration C_o
t = time (min.)
V_{int} = total particle internal volume (ml.)
Z = axial distance in bed (cm.)

LITERATURE CITED

1. Asher, D., and D. W. Simpson, *J. Phys. Chem.*, **60**, 518 (1956).
2. Furnas, C. C., *Bureau of Mines Bulletin 361* (1932).
3. Gilliland, E. R., and R. F. Baddour, *Ind. Eng. Chem.*, **45**, 330 (1953).
4. Hiester, N. K., and Theodore Vermeulen, *Chem. Eng. Progr.*, **48**, 505 (1952).
5. Hougen, O. A., and K. M. Watson, "Chemical Process Principles," Vol. 3, Wiley, New York (1947).
6. Kunin, Robert, "Ion Exchange Resins," 2 ed., p. 14, Wiley, New York (1958).
7. Miner, C. S., and N. N. Dalton, "Glycerol," Reinhold, New York (1953).
8. Nachod, F. C., and J. A. Schubert, "Ion Exchange Technology," Chap. 7, Academic Press, New York (1956).
9. *Ibid.*, p. 190.
10. Opler, A., and N. K. Hiester, "Tables for Predicting the Performance of Fixed Bed Ion Exchange and Similar Mass Transfer Processes," Stanford Research Institute, Stanford, California (1954).
11. Prielipp, C., and M. Keller, *Am. Oil Ch. S. Journal*, **33**, 103 (1956).
12. Schuman, T. E., *J. Franklin Inst.*, **208**, 405 (1929).
13. Shurts, E. L., and R. R. White, *A.I.Ch. E. Journal*, **3**, 183 (1957).
14. Simpson, D. W., and R. M. Wheaton, *Chem. Eng. Progr.*, **50**, 45 (1954).
15. Simpson, D. W., and W. C. Bauman, *Ind. Eng. Chem.*, **46**, 1958 (1954).
16. Tayyabkhan, M. T., Ph.D. dissertation, Univ. Michigan, Ann Arbor, Michigan (1959).
17. Vassiliou, Basil, Thesis, National Technical University of Athens, Greece (1957).
18. Vermeulen, Theodore, "Advances in Chemical Engineering," Vol. 2, p. 147, *Academic Press*, New York (1958).
19. ———, and N. K. Hiester, *Ind. Eng. Chem.*, **44**, 636 (1952).
20. Wheaton, R. M., and W. C. Bauman, *ibid.*, **45**, 228 (1953).

Manuscript received June 13, 1961; revision received October 17, 1961; paper accepted October 18, 1961. Paper presented at A.I.Ch.E. Lake Placid meeting.

Fundamental Aspects of Rotating Disk Contactor Performance

C. P. STRAND, R. B. OLNEY, and G. H. ACKERMAN
Shell Development Company, Emeryville, California

The principles used in analyzing the performance of rotating disk contactor liquid extraction columns are discussed. The behavior of a swarm of drops in the rotating field is found to be adequately represented in most respects by single-drop dynamics, which leads to tested relations for countercurrent capacity, limiting drop holdup, axial diffusion of the continuous and dispersed phases, and point mass transfer coefficients that are independent of column size effects.

The rotating disk contactor (RDC) was introduced several years ago (*20*) and has been applied successfully in a number of liquid-liquid extraction applications. These include lube oil and gas oil extractions, propane deasphalting, sulfur dioxide extraction of kerosene fractions, solutizer treating, recovery of phenol from effluents, extraction of catalytic reformates, and miscellaneous chemicals and specialties applications. Various data for this device have been published (*5, 13, 16, 20, 22, 32*), but a comprehensive analysis of all such data has not been presented heretofore. The present work is an attempt to do this, with first principles wherever possible. The intent is to show the extent to which these principles have been verified and to outline the design philosophy that has evolved, without going into the details of the design procedure. The important assumptions and limitations are illustrated, and the concepts that require further study and verification are mentioned. The methods have been used to achieve a successful scale-up in several cases.

The RDC consists of a number of rotating disks supported on a shaft, the disks being centered between stator rings which form the compartments (*20*). A sketch of the apparatus is shown in Figure 1. The variables that must be selected for a design include the column diameter, the rotor disk diameter, the rotational speed, the diameter of the stator opening, the compartment height, and the number of compartments. When two immiscible phases are present, in countercurrent extraction, then the drop size and the amount of the drop phase in the contact zone are governed mainly by the rotor speed. A low speed results in large drops which rise rapidly through the contact zone, thereby permitting high throughputs but giving small interfacial areas and low mass transfer rates. A high rotor speed gives very small approximately spherical drops which revolve many times within a compartment along toroidal paths. This leads to lower column capacity but gives high mass transfer rates because of the increased interfacial area.

In addition to increasing the dispersed-phase holdup and the interfacial area an increase in rotor speed causes an increase in axial mixing of each phase. The two main components of the axial diffusion process are an eddy diffusion or backmixing, most pronounced at highest speeds, and a channeling or Taylor type of diffusion (*27*) which is specific in the forward direction. Axial mixing, when present